# Optical design for the Giant Magellan Telescope Multi-object Astronomical and Cosmological Spectrograph (GMACS): design methodology, issues, and trade-offs

Rafael A. S. Ribeiro*[a], Damien Jones[b], Luke M. Schmidt[c], Keith Taylor[d], Erica Cook[c], Darren L. DePoy[c], Daniel Faes[a], Cynthia Froning[c], Tae-Geun Ji[e] Hye-In Lee[e] Jennifer L. Marshall[c], Claudia Mendes de Oliveira[a], Soojong Pak[e] Casey Papovich[c], Travis Prochaska[c], Aline Souza[a]

[a]Department of Astronomy, IAG, Universidade de São Paulo (USP), São Paulo, Brazil
[b]Prime Optics, Australia; Department of Astronomy, C1400
[c]Department of Physics and Astronomy, Texas A&M University, 4242 TAMU, College Station, TX, 77843-4242 USA
[d]Instruments4, CA 91011, USA
[e]Kyung Hee University, Republic of Korea

## ABSTRACT

We present the current optical design of GMACS, a multi-object wide field optical spectrograph currently being developed for the Giant Magellan Telescope, a member of the emerging generation of Extremely Large Telescopes (ELTs). Optical spectrographs for ELTs have unique design challenges and issues. For example, the combination of the largest practical field of view and beam widths necessary to achieve the desired spectral resolutions force the design of seeing limited ELT optical spectrographs to include aspheric lenses, broadband dichroics, and volume phase holographic gratings - all necessarily very large. We here outline details of the collimator and camera subsystems, the design methodology and trade-off analyses used to develop the collimator subsystem, the individual and combined subsystem performances and the predicted tolerances.

**Keywords:** Giant Magellan Telescope, Extremely Large Telescopes, Spectrograph, GMACS, Multi-object

## 1. INTRODUCTION

The Giant Magellan Telescope (GMT) is a 25-meter effective aperture optical/infrared telescope, a member of the next generation of extremely large telescopes (ELTs). GMT is being constructed by an international consortium of universities and research institutions.[1,2]

The Giant Magellan Telescope Multi-object Astronomical and Cosmological Spectrograph (GMACS) is a first light instrument for the GMT. It will be capable of obtaining spectroscopy of ultra-faint targets that are currently identified only from broad-band imaging observations. High throughput, simultaneous wide wavelength coverage, accurate and precise sky subtraction, moderate resolution, multi-object capabilities, relatively wide field, and substantial multiplexing are crucial design drivers for the instrument. It is expected that GMACS will form one of the most important and heavily utilized scientific capabilities of the GMT.[3] it is currently being designed by a collaboration consisting of scientists and engineers from Texas A&M University, the University of Texas at Austin, University of São Paulo, Kyung Hee University, and Arizona State University.

GMACS' most recent optical design consists of a double-beam optical spectrograph comprising a split collimator, a dichroic beam-splitter, a set of volume-phase holographic transmission gratings (VPHGs) as the disperser, a set of passband filters for waveband selection, and the twin optimized f/2.2 CCD cameras.

The collimator generates an image of the telescope entrance pupil, located at its primary multiple mirror system, in the vicinity of the center of the VPHG. The pupil aberrations must be controlled due to the strong astigmatism and field curvature so as not to overload the corrections needed by the cameras. The convex radius

*rafael.alves.ribeiro@usp.br, phone: +55-16-99724-8887; http://www.iag.usp.br/astronomia/

of curvature of the telescope focal plane is ≈2,200mm formed at f/8.16 giving an image diameter of ≈450 mm for a 7.5 arcminute field of view (FoV).[4,5]

GMACS is currently in conceptual design and will undergo a midpoint conceptual design review in July of 2018 with the full conceptual design review the following March.

The paper is structured as follow: Sec.2 outlines the methodology adopted for the optical design optimization process; Sec.3 describes the requirements and the determination of the first-order optical parameters which will guide the optical design development; Sec.4 reports on three trade studies for the selection of the collimator architecture, collimator layout and control of the astigmatism caused by the dichroic and Sec.7 describes variations of the single collimator system that has commensurate high UV-blue throughput.

## 2. METHODOLOGY

The methodology adopted for the development of the GMACS optical system is an applied case of the general optical design for an astronomical spectrograph. It has three progressive stages of optimization, Fig.1.

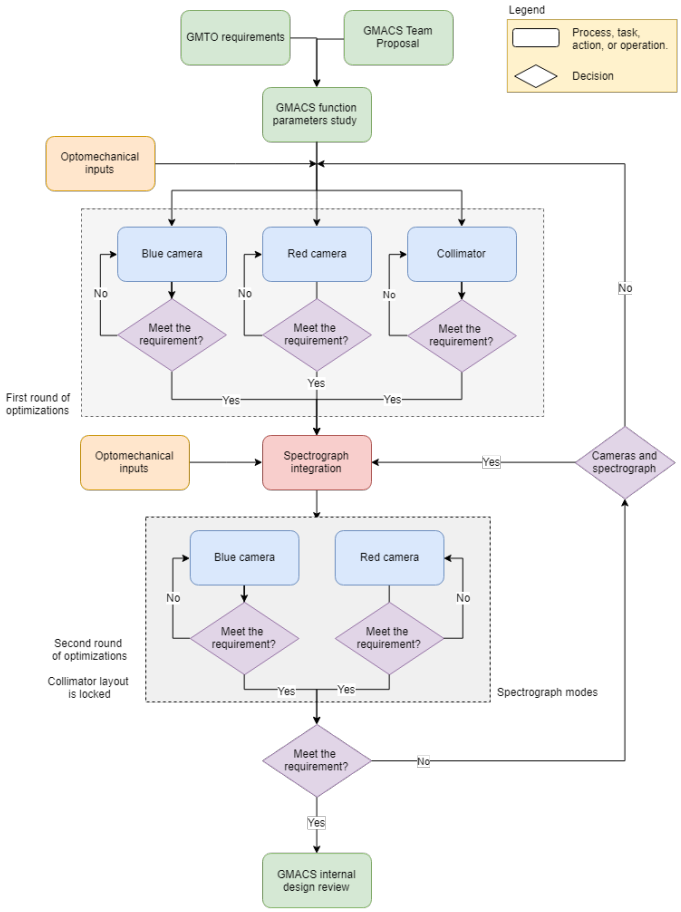


Figure 1: Diagram flowchart of the methodology used for the GMACS optical system.

The first is related to the definition of the optical functional parameters for the spectrograph and its subsystems. The inputs are the instrument requirements, suppliers capabilities for manufacturing key components, the recommended solution from former similar instruments and stakeholder needs. The output is a consolidated set of functional parameters of the instrument optical design.

Once the requirements are well defined, the second stage starts with the determination of the subsystem's functional parameters followed by re-optimization tests. This stage includes several trade-off analyses including architectures and technical solutions that have been selected. It is expected that supporting studies are carried out during this stage including sensitivity tolerancing and instrument flexures.

The third stage involves the integrated optical design optimization from the selection of the chosen subsystems. This stage considers grating effects and the peculiarities in the merit functions for the spectrograph. It is common that the second and third stages are circular in nature and require several iterations.

## 3. GMACS REQUIREMENTS

Through collaboration with the Giant Magellan Telescope Organization (GMTO), its partners and other representatives from the scientific community, a set of principal functional requirements have been developed. A 2014 GMACS community workshop included more than 50 participants from GMT partner and non-partner institutions with broad scientific interests. The recommendations of this meeting were integrated into the GMACS scientific requirements and flowed down to the definition of the GMACS functional parameters. The image quality requirement is tied to future integration with MANIFEST, the GMT fiber positioner which can be used in conjunction with GMACS to access the full 20 arcminute diameter field of view of the GMT.

Table 1: GMACS Principal Functional Parameters.

| **Parameter** | **Requirement** | **Goal** |
|---|---|---|
| Field of View | 30 arcmin sq. | 50 arcmin sq. |
| Wavelength Coverage | 350-950nm | 320-1000nm |
| Spectral Resolution | Blue: 1000-6000, Red 1000-6000 | Blue: 1000-6000, Red 1000-6000 |
| Image Quality | 80% EE at 0.30 arcsec | 80% EE at 0.15 arcsec |
| Spectral Stability | 0.3 spectral resolution elements/hour | 0.1 spectral resolution elements/hour |
| Number of Gratings | 2 | $\geq 2$ |
| Slit Mask Exchange | 12 | $\geq 20$ |

The wavelength coverage for high resolution mode may be sacrificed, but full coverage is required at lower resolution. The spectral stability is mainly affected by flexure due to the gravity and temperature variations.

## 4. TRADE-OFF ANALYSIS

This section describes three examples of trade studies for the selection of the collimator architecture, collimator layout and control of the astigmatism caused by the dichroic.

### 4.1 Collimator architectures

The trade-off for the determination of the collimator architecture has two levels, Fig.2. The first referred to as "conceptual trade-off" is for the identification of the collimator concepts appropriate to the requirements. Their advantages, disadvantages and high-level performance criteria are used as inputs for the second "architectural trade-off". This gathers more detailed information such as estimated image quality, material constraints, difficulties in mounting, and sensitivities to flexure.

The following concepts comply with the same parameters described by Schmidt et.al. (2016)[4] : $f/8.16$, 2,200mm effective focal length and field of view (FoV) of 11.6° with a GMACS FoV diameter of 7.4 arcmin.

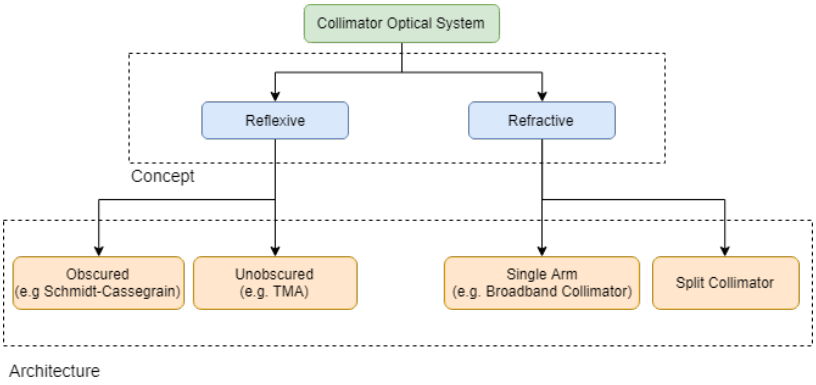


Figure 2: Collimator trade-off.

Table 2: Advantages and disadvantages for reflective collimators

| | Obscured | Unobscured |
|---|---|---|
| **Advantages** | No wavelength dependence<br>Good image quality<br>High overall transmittance<br>High UV-Blue transmittance | No wavelength dependence<br>Good image quality<br>High overall throughput<br>High UV-Blue throughput |
| **Disadvantages** | Field vignetting<br>Hard to design for large FoV (≈11°)<br>Challenging alignment and stability | Size and packaging constraints<br>Challenging alignment<br>Large freeform mirrors |

### 4.1.1 Reflective concept

The two sets of reflective collimator architectures considered are the obscured type, such as a Schmidt-Cassegrain and the unobscured type such as Three Mirror Anastigmatic (TMA). Tab.2 briefly shows a summary of the advantages and disadvantages of these architectures applied for GMACS.

The main advantages for the reflective collimator concepts are the good image quality, the expected high throughput in the UV-blue spectral range which follows the same spectral performance of the GMT mirrors, and the intrinsic achromaticity of reflective optical systems. However, the disadvantages such as field vignetting, packaging constraints and alignment challenges are considered detrimental and cause high negative impact on the instrument development.

### 4.1.2 Refractive concept

The curvature of the GMT focal plane, concave towards the instrument, is an advantage for a refractive collimator as it ensures that the collimator group remains small. Tab.3 summarizes the advantages and disadvantages of the refractive architecture.

Table 3: Advantage and disadvantages for refractive collimators

| | |
|---|---|
| **Advantages** | Large FoV<br>Smaller packaging<br>More degrees of freedom for optimization<br>Straightforward to align |
| **Disadvantages** | Fewer glasses available for large optics<br>Glass tends to absorbs UV-Blue |

#### 4.1.3 Collimator architecture conclusion

Both a reflective and refractive collimator architectures are compliant with the GMACS image quality requirements. However, the size, packaging constraints, alignment challenges, and stability requirements are strong negatives for the reflective architectures. Therefore, the selected architecture for GMACS is refractive.

The next section describes a trade-off study for two potential refractive collimator designs.

### 4.2 Refractive collimator architectures

The two refractive GMACS collimators presented in this work are most notably differentiated by the location of the dichroic. The most straightforward layout has the dichroic located in the collimated beam and must be capable of operating over the entire GMACS spectral range. This collimator is referred to as the "single collimator" configuration. The alternative architecture has the dichroic located just after the field lens and requires two independent collimator subsystems, one for each spectral band. This layout is referred to as the "split collimator".

Tab.4 summarizes the advantages and disadvantages of each refractive collimator architecture.

The "single collimator" concept is the most traditional solution as compared to the other designs. However, the requirement for broad wavelength coverage is a significant design challenge due to a limited choice of glasses with available sizes and sufficient internal transmittance below 350nm. A trade-off study of three alternatives for this concept is reported in Sec.7.

The main characteristic of the split collimator is that the dichroic is located right after the field lens with the consequence that there are two independent collimator subsystems, one for each spectral range, allowing for better overall colour correction, including that of the pupil. Additionally, now the dichroic is located before the collimator group, the pupil relief can be smaller than for the single collimator, which in turn reduces the diameter of all the camera elements.

There are three drawbacks of the split collimator configuration: 1) the tilted dichroic generates astigmatism in the red arm because of its location in a diverging beam and requires an additional optical element for its compensation; 2) the blue arm requires a plane mirror to realign its optical axis parallel with the original axis (a requirement due to mechanical constraints); and 3) the collimator support is more complex and the two arms are prone to differential flexure.

Table 4: Refractive collimator architectures advantages and disadvantages

| | **Single Collimator** | **Split Collimator** |
|---|---|---|
| **Advantages** | Simple design<br>Fewer elements | Higher UV-blue throughput<br>Better color correction<br>Better exit pupil quality<br>Reduced collimator eye relief (smaller optics) |
| **Disadvantages** | Large eye relief (large optics)<br>Reduced UV-blue throughput | Astigmatism due to tilted dichroic in converging beam<br>Additional mirror is required<br>Larger mechanical packaging<br>Envelope constraints for high mode resolution |

### 4.3 Astigmatism compensator

As mentioned in the section above, the split collimator architecture has a drawback related to the tilted dichroic which generates astigmatism in the red arm because of its location in a diverging beam. The trade-off analysis to compensate it includes:

- A compensator window tilted at an axis orthogonal to the dichroic;
- Cylindrical compensator or a dichroic with a cylindrical second surface;

- A wedge dichroic and compensator.

The more traditional astigmatism corrector in this situation consists of another tilted plate but rotated by 90° around the optical axis. Unfortunately, the sheer size of the collimator field causes large, asymmetric and uncorrectable residual aberrations.

The current split-collimator design has a long radius (≈120 meters) cylindrical on the dichroic rear surface as an astigmatism compensator for the red arm, which works satisfactorily. An alternative solution, not presented in this work, uses a plano-plano dichroic and a cylindrical element with a similar long radius of curvature also works properly. However, both solution have long radius cylindrical surfaces which may be very difficult to manufacture and the additional element impacts on the throughput.

Therefore, our favoured solution for the next version is for a second plate tilted in the opposite sense to the beamsplitter. Both the beamsplitter and the second plate are given a small wedge. Besides the fact that adding element impacts on the throughput, the resultant aberrations, including lateral colour, are nearly completely symmetric and thus intrinsically correctable. This solution will also eliminate the afore-mentioned manufacturability concerns.

## 5. GMACS OPTICAL SYSTEM

For reasons highlighted above, the current GMACS optical system is based on the split collimator architecture. It uses a dual-beam Volume Phase Holographic Grating (VPHG) with a CCD mosaic as its detector. The collimator is an f/8.2, 2,200mm effective focal length imaging the GMT entrance pupil onto the grating planes while splitting the incoming light into two spectral bands corresponding to blue (320nm to 600nm) and red (500nm to 1000nm) as separated by a tilted dichroic. The dispersed beams are imaged by two independent articulated f/2.2 cameras operating in transmission Littrow. The dichroic transition is set at 557.7 nm (a bright atmospheric emission line) and the steepness of the dichroic transition will determine the spectral overlap required to generate a complete spectrum.

All the GMACS optical groups comprise singlets or air-doublets to avoid the use of cemented or coupled optics.

### 5.1 Detector

The camera focal planes are assumed to be a 2-by-3 mosaic of $4k^2$ @$15\mu m$ pixel pitch CCDs forming an effective sensor array of 12,288 x 8,192 pixels, Fig.3. The shorter dimension is assumed to be the "spatial direction" with the longer the "spectral direction".

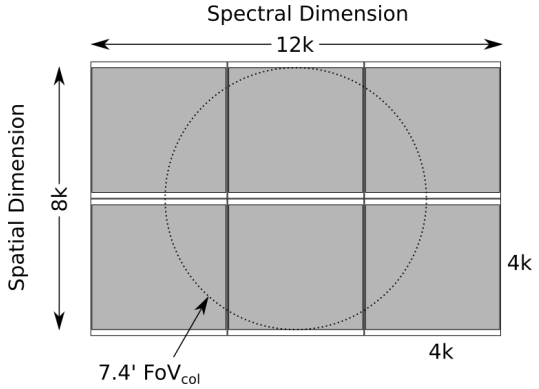


Figure 3: 12k-by-8k CCD mosaic forming the sensor assembly for the GMACS. The imaging FoV is shown by the dashed circle whose diameter is enclosed within the smaller sensor dimension. It is assumed that the dispersion direction is in the orthogonal dimension.

## 5.2 Split Collimator

A layout of the split collimator layout is illustrated in Fig.4. The fused silica field lens (FL) is the only optical element shared by both collimator arms. The dichroic splits the beams feeding the two collimator arms. For the blue arm, a plane mirror is used to comply with space constraints, with its collimator group having only FS and $CaF_2$. The red arm is fed by the transmissive beam of the dichroic with its collimator group having PBL6Y, $CaF_2$ and BSM51Y glasses. Both collimator groups have one aspherical surface, located in the element closest to the collimator exit pupil.

This design corrects the astigmatism caused by the tilted dichroic by setting the dichroic's second surface as a cylindrical surface of radius ≈122 meters. As presented in Sec.4.3, other alternatives are being explored in a specific trade-off.

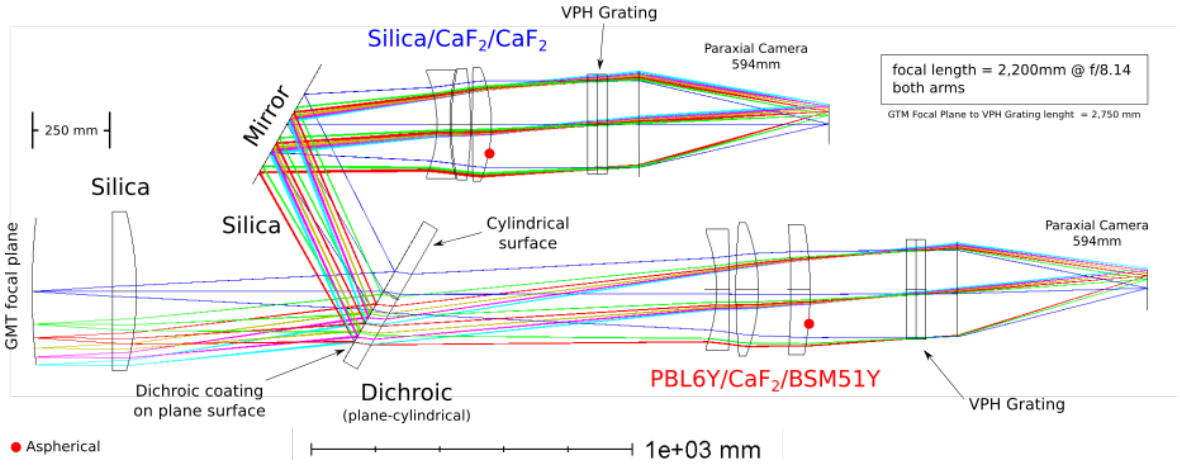


Figure 4: GMACS Split Collimator with paraxial cameras.

The throughput, excluding the dichroic coating performance and considering a 99% transmittance of the AR coating, and 95% of mirror reflectance, is $T_{blue} \approx 78\%$ and $T_{red} \approx 75\%$.

Fig.5 shows the spot diagram of the split collimator with 592mm focal length paraxial cameras for a circular FoV of 7.4 arcmin diameter. The reference circle is 0.3 arcsec diameter. All the geometric encircled energy falls in this circle. The transverse chromatic aberration is $150\mu m$ for blue and $30\mu m$ for red.

The polarization effects caused by both the dichroic and the mirror in the blue collimator is yet to be examined.

## 5.3 Cameras

### 5.3.1 Blue Camera

The blue camera is an f/2.2, 592mm effective focal length system, comprising eight elements of fused silica and $CaF_2$. The reason for this selection is due to their high internal transmission below 350nm wavelength, Fig.6. The considerations for the development this camera are shown in Tab.5.

The design controls axial color, however, it has $\approx 700\mu m$ of TCA, which is $\approx 3.6$ times the spectral resolution for a 0.7 arcsec slit. The quantitative consequences of the TCA in the spectrograph mode are still under investigation. Three aspheric surfaces on positive $CaF_2$ lenses, shown with marked with red dot in the Fig.6, can help control the field aberrations. Their deviation from best spherical fit are approximately $250\mu m$, $1,000\mu m$ and $360\mu m$, from the surfaces left to right of the Fig.6, with maximum slope of $1.5 \times 10^{-2}$, $5.0 \times 10^{-2}$ and $2.0 \times 10^{-2}$, respectively. The estimated throughput is $\approx 70\%$ throughout the blue spectral range, assuming a

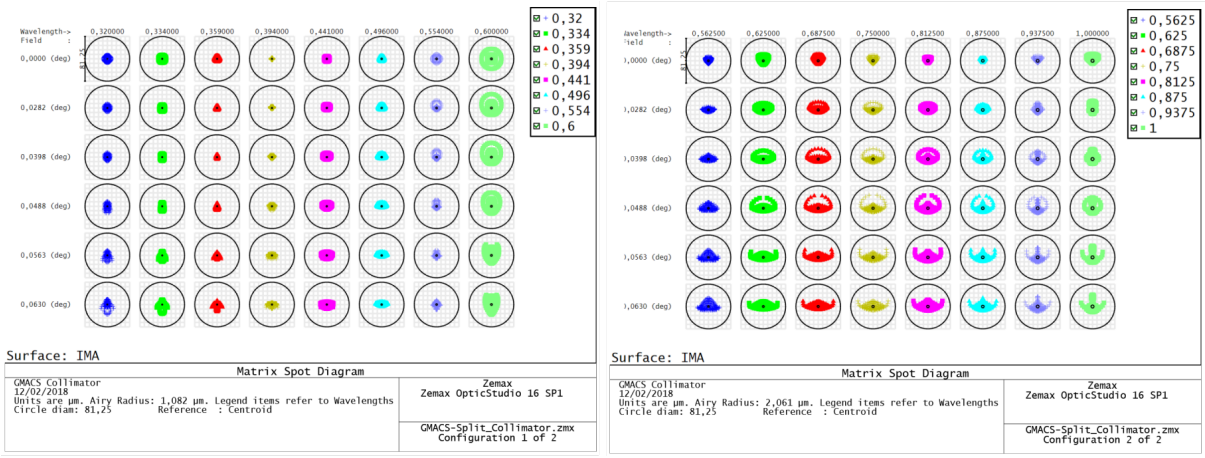


Figure 5: Spot diagram for the Split collimator with 592mm focal length paraxial cameras. **Left**: blue arm from 320nm - 600nm. **Right**: red arm from 560nm to 1.000nm. The reference circle is 0.3 arcsec diameter.

99% transmittance of the AR coating, 95% of mirror reflectance and the internal transmittance data from glasses suppliers.

The cameras have a field vignetting maximum of 10% at their extremities. However, this effect is considered negligible for low-resolution modes and acceptable for the high-resolution spectrograph modes because the field vignetting turns into spectral vignetting only for a small range at both extreme wavelengths and extreme fields. It is estimated that the worst case have less than 18% of the ray bundle vignetted.

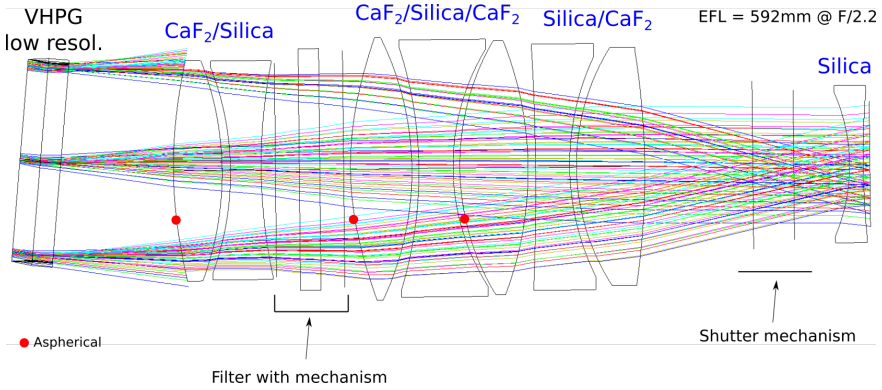


Figure 6: Blue Camera.

The next planed design modification for the blue camera is to move the filter with its mechanisms close to the shutter and to attempt to reduce the number of aspherics.

### 5.3.2 Red Camera

The red camera has similar parameters: the system is an f/2.2, 592mm effective focal length system comprising 8 lenses of fused silica, $CaF_2$, PBL6Y, BSM51Y and LAL59, Fig.7. The only aspheric surface is at the first positive $CaF_2$ with spherical deviation approximately $180\mu m$ and maximum slope of $1.1 \times 10^{-2}$. The estimated throughput is $\approx$ 73% throughout the red spectral range, assuming a 99% transmittance of the AR coatings taking the internal transmittance data from suppliers.

Table 5: Blue camera design considerations

| | |
|---|---|
| **Higher throughput requires:** | Minimize the number of air-glass interfaces;<br>Only FS+$CaF_2$ materials for the lenses (Similar to blue arm collimator to achieve higher throughput below 350 nm). |
| **Material restriction consequences:** | Difficult to get color corrections (Secondary and Transverse Chromatic Aberration(TCA));<br>Increases the number of elements to achieve acceptable performance. |
| **Avoiding cemented optics leads to:** | Increases in the number of air-glass interfaces;<br>Increases possibilities for aspherical surfaces. |
| **Vignetting effects:** | Better performance;<br>Reduced spectral flux as function of field and wavelength. |

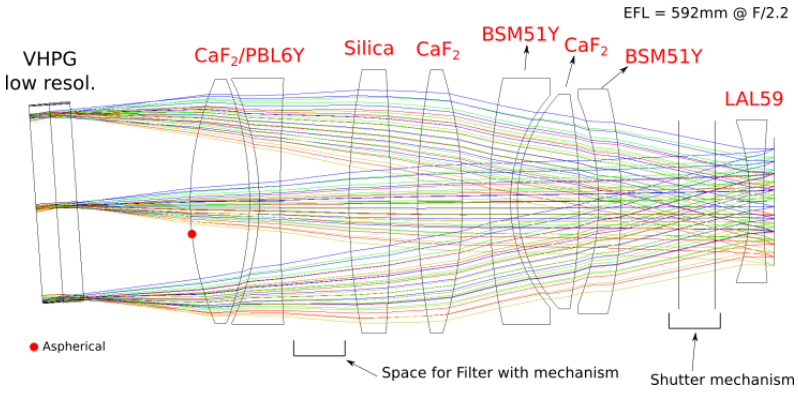


Figure 7: Red Camera.

## 6. GMACS OPERATION MODES

The presented GMACS spectrograph layout for the low and high resolution modes with the refractive split collimator are described in this section. Tab.6 shows the basic parameters for the slit, the plate scale generated by the telescope, and the parameters in common in the spectrograph modes.

Table 6: Split and spectrograph parameters

| | |
|---|---|
| **Slit width x length** | 0.7 arcsec x 7.4 arcmin<br>0.704 mm x 446.8 mm |
| **Plate Scale** | 1 arcsec/mm |
| **Anamorphic factor** | 1 |
| **Diffraction order** | 1 |
| **Pixels/slit width** | 12.6 |

### 6.1 Spectrograph modes

Fig.8 shows the GMACS layout for both resolution modes and for both arms. The GMT focal plane, FL and first surface of the dichroic are the only shared elements/surface for both arms. The first reflective surface of the blue arm represents the first dichroic surface. The dichroic, for a ray tracing purposes, is a tilted window for the red arm. The VPHG tilt direction avoid any possibility of mechanical interference.

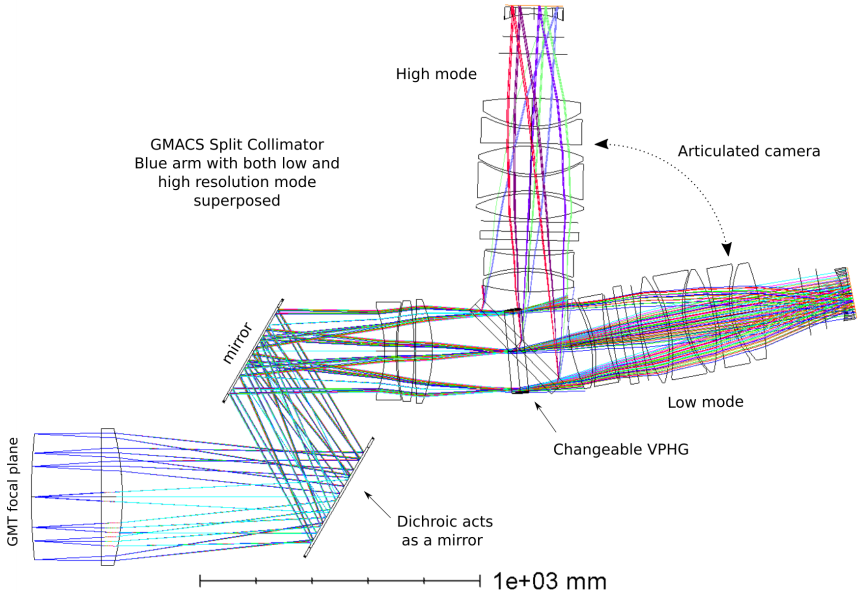


(a) GMACS blue arm

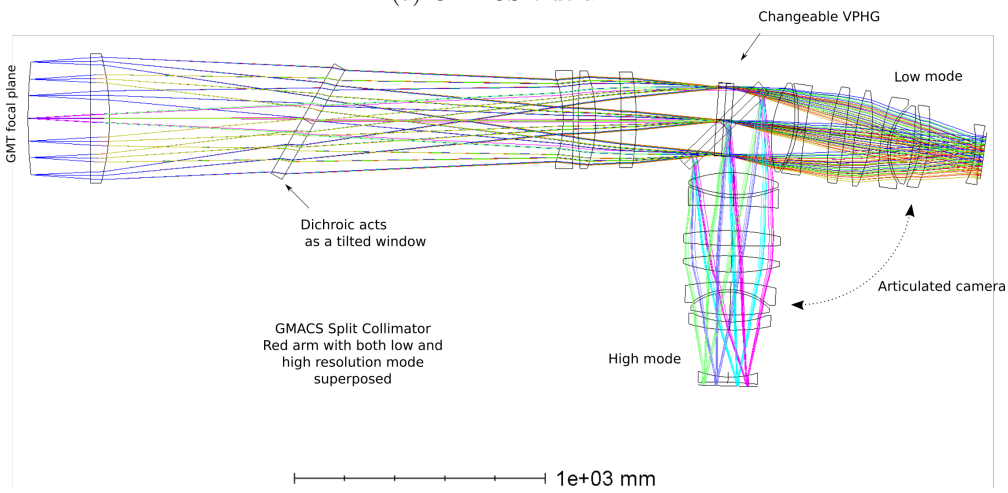


(b) GMACS red arm

Figure 8: GMACS layout for both superposed resolution modes and for both arms.

The fields of view for the low resolution mode are spread over the collimator FoV (7.4 arcmin diameter) to meet the multi-object capability for GMACS. Because the system is non-symmetrical due to the tilted dichroic and grating, the symmetrical fields are included as well. No wavelength is sacrificed for object at the collimator FoV in the low resolution mode.

The fields of view for the high resolution mode is along the orthogonal direction of the grating lines and in the center of the collimator FoV. It simulates a 7.5 arcmin long slit which direction is orthogonal in the paper plane of both Fig.8a and b. Only for the fields within the long slit have no spectral loss. For any other field the bluer or redder wavelengths of the spectral range is sacrificed.

### 6.1.1 Spectrograph performance

The spectrograph spot diagram for both resolution modes for both arms are described in Fig.9. The blue arm has an slightly better and constant performance over the spectral range.

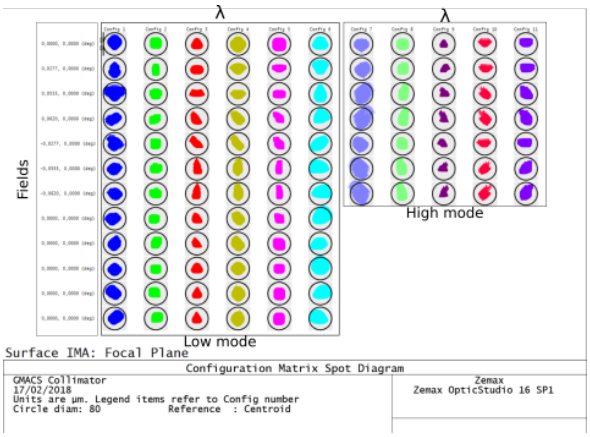


(a) Blue arm, for spectral range from 320-550nm in low resolution mode.

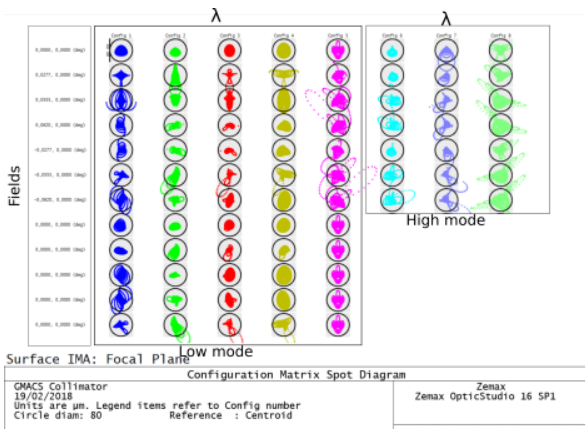


(b) Red arm, for spectral range from 550-1000nm in low resolution mode.

Figure 9: GMACS performance for both spectrograph resolution mode. The circle reference is 0.3 arcsec ($\approx 80\mu m$ at the focal plane). The spectral range for the high resolution mode is about 100nm centered in any wavelength within the low resolution mode spectral range.

### 6.2 Image mode

GMACS can provide an narrow-band imaging mode for both spectral ranges by articulating the VPHG + camera optical axis to a straight-through configuration, similar to the low resolution mode layout in Fig.8. The maximum band for the filter of which the transverse chromatic aberration is lesser than one pixel ($15\mu m$) is approximately 15-20nm.

## 7. NIKON GLASS FOR SINGLE COLLIMATOR

The availability of glasses for large refractive optical systems is considerably limited when compared to typical dimensions due to production challenges for large blanks with high optical homogeneity.[6,7]

For the GMACS system, the requirement for high throughput for wavelengths less than 350nm is an aggravating factor which further limits the solutions. The optical designer has few glass options to overcome chromatic aberrations, such as transversal and spherochromatism.

Nikons' NIGS i-line glass family has increased the number of glasses available for astronomical instrumentation application, which might serve as alternative for $CaF_2$ (NIGS 4786) while providing strong flints with high internal transmittance in bluer regions which increases the possible glass combinations. Fig.10 shows the Abbe Diagram for the glasses with blanks larger than 250mm having more than 88% internal transmittance at 320nm for a sample thickness of 10mm. Among them, the highest 320nm internal transmission are $CaF_2$, NIGS 4786, Silica and NIGS 5859. This last glass has similar optical parameters as BAL35Y and BSM51Y but higher internal transmittance for bluer wavelengths.

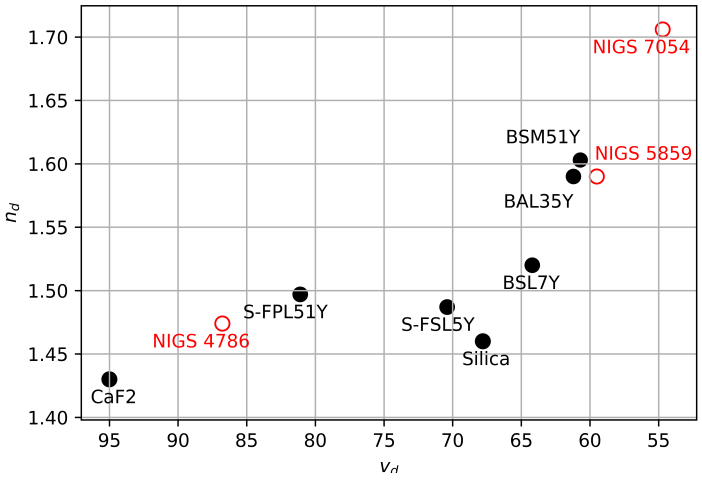


Figure 10: Abbe diagram for the blue arm optical system. The unfilled red dots are from Nikon's glass catalog of the NIGS family.

As part of the collimator architecture trade-off analysis described in Sec.4.2, we have designed three versions of the single arm collimator which differ only in the glass choice and consequent optical performance and the instrument throughput in the UV-Blue region.

The designs have the same layout concept of the split refractive architecture: a field lens (FL) followed by a collimating group. All of them are broad-band collimators to cover the full GMACS spectral range.

The difference between the first and the second versions is the flint glass of the air-doublet: Ohara BAL35Y and Nikon NIGS 5859, respectively. Fig.11 shows the design for first version. The second version has a similar layout. The main objective for the additional glass type is for better chromatic corrections. The internal transmittance for a 10mm sample thickness for the glasses are 92% for BAL35Y and 98.6% for NIGS 5859. However, the unique crucial drawback for using NIGS 5859 is that, based on our present state of suppliers informations, banks sizes around 350mm diameter area not available.

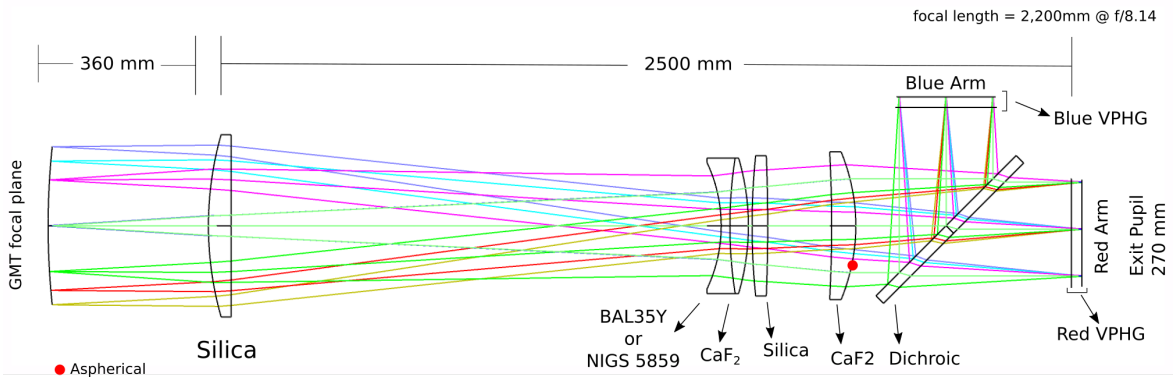


Figure 11: First and second version of the single arm collimator layout.The difference between them is the flint glass of the air-doublet: Ohara BAL35Y and Nikon NIGS 5859, respectively

The third version is a collimator based only on fused silica and $CaF_2$, Fig.12. This design has achromatic performance over the GMACS spectral range, but it is insufficient to provide acceptable image quality over all the GMACS spectral range due to the high dependence of the spherical aberration to wavelength.

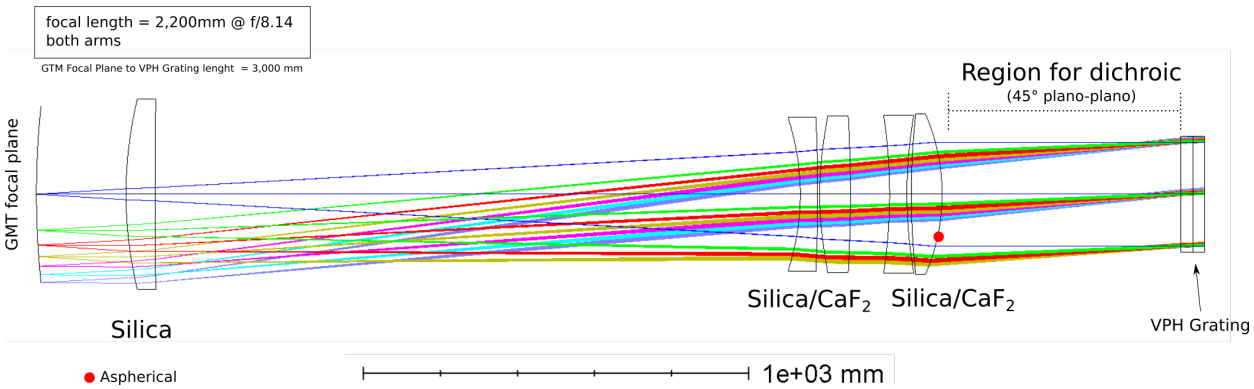


Figure 12: Single broadband collimator based on fused silica and $CaF_2$.

## 8. NEXT WORK

GMACS is currently in conceptual design and will undergo a midpoint conceptual design review in July of 2018. However, the following improvements and proposed studies listed below already were identified and will be explored before this meeting.

It will be included an additional step in the second round of optimization of the design methodology, described in Fig.1, which incorporates the respective collimator system as a variable during the spectrograph optimization processes. The principal objective is to allow both collimator and camera to compensate each other color and fields aberration without compromise the spectral image quality.

Regarding the blue arm of the split collimator design, a detailed study is required to quantify the influence of the tilted mirror in a possible GMACS polarimetric mode provided by MANIFEST. For the blue camera, both filter and its mechanisms will be moved next to the shutter and the focal plane, which will favor the camera group stiffness and probably allows the removal of an aspheric surface.

As cited in Sec.4.3, the wedge dichroic and compensator solution to correct the astigmatism caused by the tilted dichroic will be implemented in the red arm of the split collimator. For the red camera, the glass material of the field flattener will be changed to fused silica, because there is a concerning of the LAL59 quality degradation under cosmic rays incidence. Finally, the overall glass selection will be refined.

## ACKNOWLEDGMENTS

GMT Brazilian Office, thought Fundação do Amparo à Pesquisa do Estado de São Paulo, FAPESP, for the financial supporting and Texas A&M University thanks Charles R. '62 and Judith G. Munnerlyn, George P. '40 and Cynthia Woods Mitchell, and their families for support of astronomical instrumentation activities in the Department of Physics and Astronomy.

## REFERENCES

1. M. Johns, P. McCarthy, K. Raybould, A. Bouchez, A. Farahani, J. Filgueira, G. Jacoby, S. Shectman, and M. Sheehan, "Giant Magellan Telescope: overview," in *Proc. SPIE 8444*, L. M. Stepp, R. Gilmozzi, and H. J. Hall, eds., 2012.
2. P. J.McCarthy, J. Fanson, R. Bernstein, D. Ashby, B. Bigelow, N. Boyadjian, A. Bouchez, E. Chauvin, E. Donoso, J. Filgueira, R. Goodrich, F. Groark, G. Jacoby, and E. Pearce, "Overview and status of the giant magellan telescope project," *Proc. SPIE 9906, Ground-based and Airborne Telescopes VI* **9906**, p. 990612, 2016.

3. D. L. DePoy, R. Allen, R. Barkhouser, E. Boster, D. Carona, A. Harding, R. Hammond, J. L. Marshall, J. Orndorff, C. Papovich, K. Prochaska, T. Prochaska, J. P. Rheault, S. Smee, S. Shectman, and S. Villanueva, "GMACS: a wide field, multi-object, moderate-resolution, optical spectrograph for the Giant Magellan Telescope," in *Proc. SPIE 8446, Ground-based and Airborne Instrumentation for Astronomy IV*, **8446**, 2012.
4. L. M. Schmidt, R. Ribeiro, K. Taylor, D. Jones, T. Prochaska, D. L. DePoy, J. L. Marshall, E. Cook, C. Froning, T.-G. Ji, H.-I. Lee, C. M. de Oliveira, S. Pak, and C. Papovich, "Optical design concept for the Giant Magellan Telescope Multi-object Astronomical and Cosmological Spectrograph (GMACS)," *Proc.SPIE* **9908**, 2016.
5. T. Prochaska, M. Sauseda, J. Beck, L. Schmidt, E. Cook, D. L. DePoy, J. L. Marshall, R. Ribeiro, K. Taylor, D. Jones, C. Froning, S. Pak, C. M. de Oliveira, C. Papovich, T.-G. Ji, and H.-I. Lee, "Optomechanical design concept for the Giant Magellan Telescope Multi-object Astronomical and Cosmological Spectrograph (GMACS," *Proc.SPIE* **9908**, 2016.
6. R. Jedamzik, J. Hengst, F. Elsmann, C. Lemke, T. Döhring, and P. Hartmann, "Optical materials for astronomy from SCHOTT: the quality of large components," *Proc.SPIE* **7018**, 2008.
7. R. Jedamzik, U. Petzold, Volker, Dietrich, V. Wittmer, and O. Rexius, "Large optical glass blanks for the ELT generation," *Proc.SPIE* **9912**, 2016.